Using 2 $\rightarrow$ 3 exclusive processes as a channel to probe generalised parton distributions

QCD Master Class 2023

Saad Nabeebaccus
IJCLab

June 13, 2023

Based on 2212.00655, 2302.12026 and work in progress with S. Wallon, L. Szymanowski, B. Pire, G. Duplančić, K. Passek-Kumerički, N. Crnković

- DIS: inclusive process *(forward amplitude)*

  $x \Rightarrow$ 1-dimensional structure

  Coefficient Function (hard) $\otimes$ Parton Distribution Function (soft)

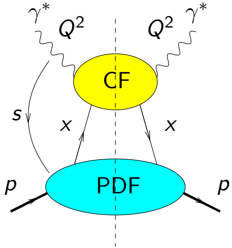

- DIS: inclusive process *(forward amplitude)*

  $x \Rightarrow$ 1-dimensional structure

  Coefficient Function $\otimes$ Parton Distribution Function
  (hard) (soft)

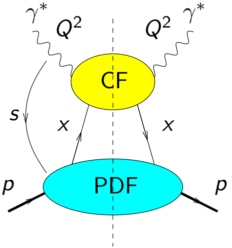

- DVCS: exclusive process (non-forward amplitude)

  (DVCS: Deeply Vitual Compton Scattering)

  Fourier transf.: $t \leftrightarrow$ impact parameter

  $(x,\ t) \Rightarrow$ 3-dimensional structure

  Coefficient Function $\otimes$ Generalized Parton Distribution
  (hard) (soft)

  Müller et al. '91 - '94; Radyushkin '96; Ji '97

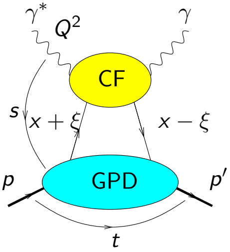

- Meson production: γ replaced by $\rho,\ \pi, \cdots$

GPD (soft) $\otimes$ CF (hard) $\otimes$ Distribution Amplitude (soft)

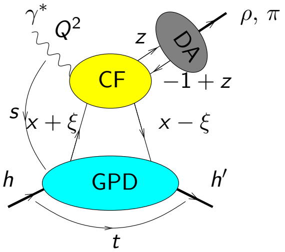

Collins, Frankfurt, Strikman '97; Radyushkin '97

proof of factorisation valid only for some restricted cases

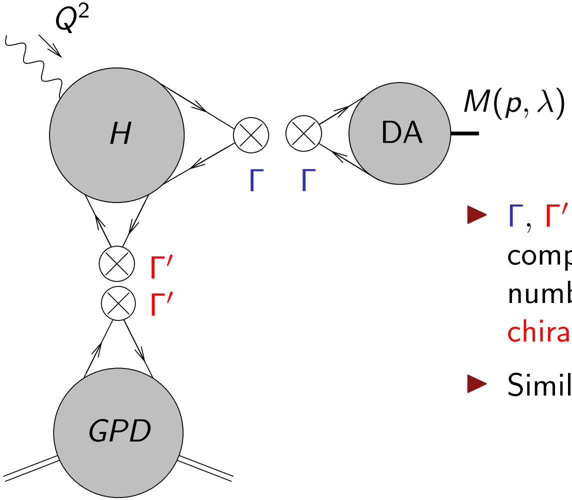

- Γ, Γ': Dirac matrices compatible with quantum numbers: C, P, T, chirality
- Similar structure for colour

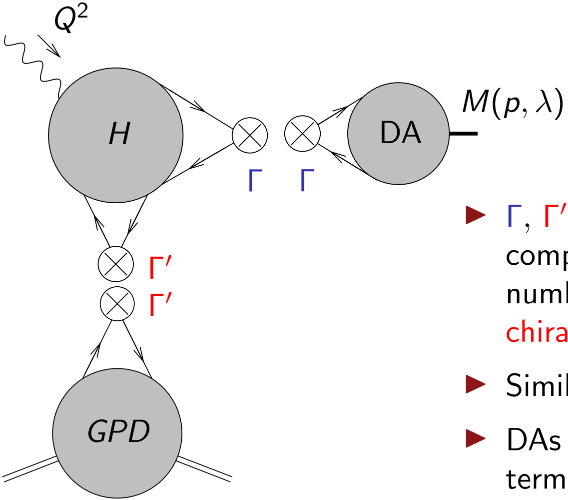

- Γ, Γ': Dirac matrices compatible with quantum numbers: C, P, T, chirality
- Similar structure for colour
- DAs and GPDs ordered in terms of twist

Quark GPDs at twist 2 [Diehl: hep-ph/0307382]

without helicity flip (chiral-even Γ matrices): 4 chiral-even GPDs:
(Note: $\Delta = p' - p$)

$$\begin{aligned} F^q &= \frac{1}{2}\int \frac{dz^-}{2\pi}\, e^{ixP^+z^-} \langle p'|\, \bar{q}(-\tfrac{1}{2}z)\, \gamma^+ q(\tfrac{1}{2}z)\, |p\rangle \Big|_{z^+=0,\, z_\perp=0} \\ &= \frac{1}{2P^+}\left[H^q(x,\xi,t)\, \bar{u}(p')\gamma^+ u(p) + E^q(x,\xi,t)\, \bar{u}(p')\frac{i\,\sigma^{+\alpha}\Delta_\alpha}{2m} u(p) \right], \end{aligned}$$

Quark GPDs at twist 2 [Diehl: hep-ph/0307382]

without helicity flip (chiral-even Γ matrices): 4 chiral-even GPDs:
(Note: $\Delta = p' - p$)

$$F^q = \frac{1}{2}\int \frac{dz^-}{2\pi}\, e^{ixP^+z^-} \langle p'|\, \bar{q}(-\tfrac{1}{2}z)\, \gamma^+ q(\tfrac{1}{2}z)\, |p\rangle \Big|_{z^+=0,\, z_\perp=0}$$
$$= \frac{1}{2P^+}\left[H^q(x,\xi,t)\, \bar{u}(p')\gamma^+ u(p) + E^q(x,\xi,t)\, \bar{u}(p')\frac{i\,\sigma^{+\alpha}\Delta_\alpha}{2m} u(p)\right],$$

$$\tilde{F}^q = \frac{1}{2}\int \frac{dz^-}{2\pi}\, e^{ixP^+z^-} \langle p'|\, \bar{q}(-\tfrac{1}{2}z)\, \gamma^+\gamma_5\, q(\tfrac{1}{2}z)\, |p\rangle \Big|_{z^+=0,\, z_\perp=0}$$
$$= \frac{1}{2P^+}\left[\tilde{H}^q(x,\xi,t)\, \bar{u}(p')\gamma^+\gamma_5 u(p) + \tilde{E}^q(x,\xi,t)\, \bar{u}(p')\frac{\gamma_5\,\Delta^+}{2m} u(p)\right].$$

Quark GPDs at twist 2 [Diehl: hep-ph/0307382]

without helicity flip (chiral-even Γ matrices): 4 chiral-even GPDs:
(Note: $\Delta = p' - p$)

$$F^q = \frac{1}{2}\int \frac{dz^-}{2\pi}\, e^{ixP^+z^-} \langle p'|\, \bar{q}(-\tfrac{1}{2}z)\, \gamma^+ q(\tfrac{1}{2}z)\, |p\rangle \Big|_{z^+=0,\, z_\perp=0}$$
$$= \frac{1}{2P^+}\left[H^q(x,\xi,t)\, \bar{u}(p')\gamma^+ u(p) + E^q(x,\xi,t)\, \bar{u}(p')\frac{i\,\sigma^{+\alpha}\Delta_\alpha}{2m} u(p)\right],$$

$$\tilde{F}^q = \frac{1}{2}\int \frac{dz^-}{2\pi}\, e^{ixP^+z^-} \langle p'|\, \bar{q}(-\tfrac{1}{2}z)\, \gamma^+\gamma_5\, q(\tfrac{1}{2}z)\, |p\rangle \Big|_{z^+=0,\, z_\perp=0}$$
$$= \frac{1}{2P^+}\left[\tilde{H}^q(x,\xi,t)\, \bar{u}(p')\gamma^+\gamma_5 u(p) + \tilde{E}^q(x,\xi,t)\, \bar{u}(p')\frac{\gamma_5\,\Delta^+}{2m} u(p)\right].$$

$H^q \xrightarrow{\xi=0,t=0}$ PDF q $\qquad$ $\tilde{H}^q \xrightarrow{\xi=0,t=0}$ polarised PDF Δq

with helicity flip (chiral-odd Γ matrices): 4 chiral-odd GPDs:

$$\frac{1}{2}\int \frac{dz^-}{2\pi}\, e^{ixP^+z^-} \langle p'|\, \bar{q}(-\tfrac{1}{2}z)\, i\,\sigma^{+i}\, q(\tfrac{1}{2}z)\ |p\rangle\Big|_{z^+=0,\, z_\perp=0}$$

$$= \frac{1}{2P^+}\bar{u}(p')\left[H_T^q\, i\sigma^{+i} + \tilde{H}_T^q\, \frac{P^+\Delta^i - \Delta^+P^i}{m^2} + E_T^q\, \frac{\gamma^+\Delta^i - \Delta^+\gamma^i}{2m} + \tilde{E}_T^q\, \frac{\gamma^+P^i - P^+\gamma^i}{m}\right] u(p)\,,$$

with helicity flip (chiral-odd Γ matrices): 4 chiral-odd GPDs:

$$\frac{1}{2}\int\frac{dz^-}{2\pi}\,e^{ixP^+z^-}\langle p'|\,\bar{q}(-\tfrac{1}{2}z)\,i\,\sigma^{+i}\,q(\tfrac{1}{2}z)\;|p\rangle\Big|_{z^+=0,\,z_\perp=0}$$
$$=\frac{1}{2P^+}\bar{u}(p')\left[H_T^q\,i\sigma^{+i}+\tilde{H}_T^q\,\frac{P^+\Delta^i-\Delta^+P^i}{m^2}\right.$$
$$\left.+E_T^q\,\frac{\gamma^+\Delta^i-\Delta^+\gamma^i}{2m}+\tilde{E}_T^q\,\frac{\gamma^+P^i-P^+\gamma^i}{m}\right]u(p)\,,$$

$H_T^q \xrightarrow{\xi=0,t=0}$ quark transversity PDFs δq

Note: $\tilde{E}_T^q(x,-\xi,t)=-\tilde{E}_T^q(x,\xi,t)$

Why consider a gamma-meson pair?
Understanding quark transversity

- Transverse spin content of the proton:

$$\begin{array}{ccc} |\uparrow\rangle_{(x)} & \sim & |\rightarrow\rangle + |\leftarrow\rangle \\ |\downarrow\rangle_{(x)} & \sim & |\rightarrow\rangle - |\leftarrow\rangle \\ \text{spin along } x & & \text{helicity states} \end{array}$$

- Observables which are sensitive to helicity flip thus give access to transversity PDFs. Poorly known.

- Transverse spin content of the proton:

$$\begin{array}{ccc} |\uparrow\rangle_{(x)} & \sim & |\rightarrow\rangle + |\leftarrow\rangle \\ |\downarrow\rangle_{(x)} & \sim & |\rightarrow\rangle - |\leftarrow\rangle \\ \text{spin along } x & & \text{helicity states} \end{array}$$

- Observables which are sensitive to helicity flip thus give access to transversity PDFs. Poorly known.

- Transversity GPDs are completely unknown experimentally.

Why consider a gamma-meson pair?
Understanding quark transversity

- Transverse spin content of the proton:

$$\begin{array}{ccc} |\uparrow\rangle_{(x)} & \sim & |\rightarrow\rangle + |\leftarrow\rangle \\ |\downarrow\rangle_{(x)} & \sim & |\rightarrow\rangle - |\leftarrow\rangle \\ \text{spin along } x & & \text{helicity states} \end{array}$$

- Observables which are sensitive to helicity flip thus give access to transversity PDFs. Poorly known.

- Transversity GPDs are completely unknown experimentally.
- For massless (anti)particles, chirality = (-)helicity
- Transversity GPDs can thus be accessed through chiral-odd Γ matrices.

- Transverse spin content of the proton:

$$
\begin{array}{ccc}
|\uparrow\rangle_{(x)} & \sim & |\rightarrow\rangle + |\leftarrow\rangle \\
|\downarrow\rangle_{(x)} & \sim & |\rightarrow\rangle - |\leftarrow\rangle \\
\text{spin along } x & & \text{helicity states}
\end{array}
$$

- Observables which are sensitive to helicity flip thus give access to transversity PDFs. Poorly known.

- Transversity GPDs are completely unknown experimentally.
- For massless (anti)particles, chirality = (-)helicity
- Transversity GPDs can thus be accessed through chiral-odd Γ matrices.
- Since (in the massless limit) QCD and QED are chiral-even $(\gamma^\mu, \gamma^\mu\gamma^5)$, the chiral-odd quantities $(1, \gamma^5, [\gamma^\mu, \gamma^\nu])$ which one wants to measure should appear in pairs.

Why consider a gamma-meson pair?
Can we probe quark transversity GPDs in DVMP?

- the leading DA (twist 2) of ρ_T is chiral-odd ($\sigma^{\mu\nu}$ coupling)

- the leading DA (twist 2) of ρ_T is chiral-odd ($\sigma^{\mu\nu}$ coupling)
- unfortunately $\gamma^* N \to \rho_T N' = 0$, since such a process would require a helicity transfer of 2 from a photon. [Diehl, Gousset, Pire: hep-ph/9808479], [Collins, Diehl: hep-ph/9907498]

- the leading DA (twist 2) of ρ_T is chiral-odd ($\sigma^{\mu\nu}$ coupling)
- unfortunately $\gamma^* N \to \rho_T N' = 0$, since such a process would require a helicity transfer of 2 from a photon. [Diehl, Gousset, Pire: hep-ph/9808479], [Collins, Diehl: hep-ph/9907498]
- lowest order diagrammatic argument:

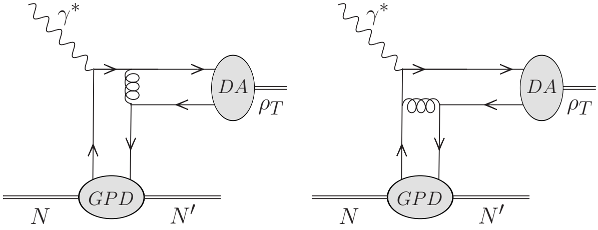

$$\gamma^\alpha[\gamma^\mu, \gamma^\nu]\gamma_\alpha = 0$$

Why consider a gamma-meson pair?
Go to higher twist?

- This vanishing only occurs at twist 2
- At twist 3 this process does not vanish [Ahmad, Goldstein, Liuti: 0805.3568], [Goloskokov, Kroll: 1106.4897, 1310.1472]

Why consider a gamma-meson pair?
Go to higher twist?

- This vanishing only occurs at twist 2
- At twist 3 this process does not vanish [Ahmad, Goldstein, Liuti: 0805.3568], [Goloskokov, Kroll: 1106.4897, 1310.1472]
- However processes involving twist 3 DAs may face problems with factorisation (end-point singularities)

  $\Rightarrow$ can be made safe in the high-energy k_T-factorisation approach

  [Anikin, Ivanov, Pire, Szymanowski, Wallon: 0909.4090]

Why consider a gamma-meson pair?

A convenient alternative solution

Circumvent this using 3-body final states:

- $\gamma N \to MMN'$:

  El Beiyad, Enberg, Ivanov, Pire, Segond, Szymanowski, Teryaev, Wallon: [1001.4491, hep-ph/0601138, hep-ph/0209300]

- $\gamma N \to \gamma MN'$:

  Boussarie, Duplančić, SN, Passek-Kumerički Pire, Szymanowski, Wallon: [1609.03830, 1809.08104, 2212.00655, 2302.12026]

Why consider a gamma-meson pair?
A convenient alternative solution

Circumvent this using 3-body final states:

- $\gamma N \to MMN'$:
  El Beiyad, Enberg, Ivanov, Pire, Segond, Szymanowski, Teryaev, Wallon: [1001.4491, hep-ph/0601138, hep-ph/0209300]
- $\gamma N \to \gamma MN'$:
  Boussarie, Duplančić, SN, Passek-Kumerički Pire, Szymanowski, Wallon: [1609.03830, 1809.08104, 2212.00655, 2302.12026]

Also many others that are not sensitive to chiral-odd GPDs:

- $\gamma N \to \gamma\gamma N'$:
  Grocholski, Pedrak, Pire, Sznajder, Szymanowski, Wagner: [1708.01043, 2003.03263, 2110.00048, 2204.00396]
- $\pi N \to \gamma\gamma N'$:
  Qiu, Yu: [2205.07846]

Why consider a gamma-meson pair?
A convenient alternative solution

Circumvent this using 3-body final states:

- $\gamma N \to MMN'$:
  El Beiyad, Enberg, Ivanov, Pire, Segond, Szymanowski, Teryaev, Wallon: [1001.4491, hep-ph/0601138, hep-ph/0209300]

- $\gamma N \to \gamma MN'$:
  Boussarie, Duplančić, SN, Passek-Kumerički Pire, Szymanowski, Wallon: [1609.03830, 1809.08104, 2212.00655, 2302.12026]

Also many others that are not sensitive to chiral-odd GPDs:

- $\gamma N \to \gamma\gamma N'$:
  Grocholski, Pedrak, Pire, Sznajder, Szymanowski, Wagner: [1708.01043, 2003.03263, 2110.00048, 2204.00396]

- $\pi N \to \gamma\gamma N'$:
  Qiu, Yu: [2205.07846]

In above cases, richer kinematics allows one to probe the sensitivity of GPDs wrt x (unlike in DVCS etc) [Qiu, Yu: 2305.15397]

Why consider a gamma-meson pair?

A convenient alternative solution

- Consider the process $\gamma N \to \gamma M N'$, M =meson. Collinear factorisation of the amplitude at large $M^2_{\gamma M}$, t', and small t.

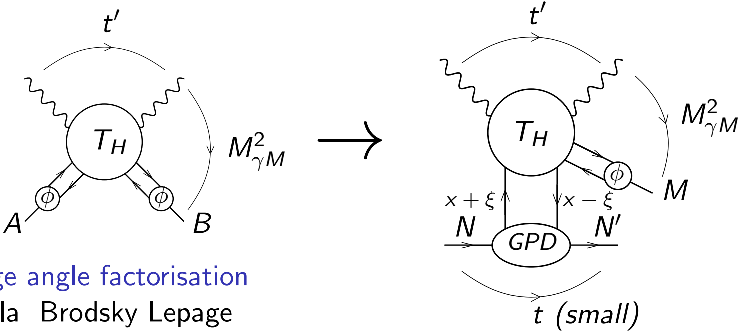

large angle factorisation
à la Brodsky Lepage

- Consider the process $\gamma N \to \gamma M N'$, $M =$meson. Collinear factorisation of the amplitude at large $M^2_{\gamma M}$, t', and small t.

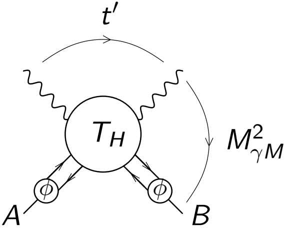

large angle factorisation
à la Brodsky Lepage

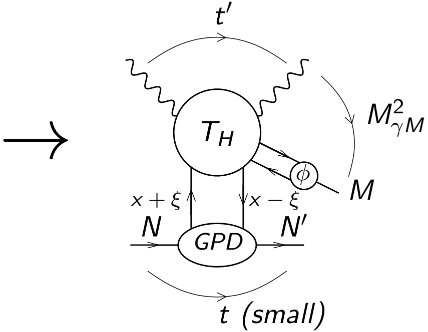

- Mesons considered in the final state: $\pi^{\pm}$, $\rho^{\pm,0}_{L,T}$.

- Consider the process $\gamma N \to \gamma M N'$, $M =$meson. Collinear factorisation of the amplitude at large $M^2_{\gamma M}$, t', and small t.

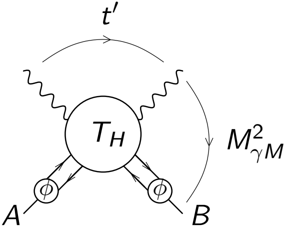

large angle factorisation
à la Brodsky Lepage

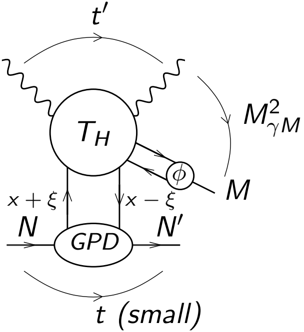

- Mesons considered in the final state: $\pi^{\pm}$, $\rho^{\pm,0}_{L,T}$.
- Leading order and leading twist

How does it work (at LO)?

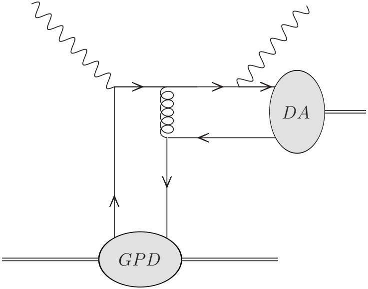

Typical non-zero diagram for a transverse ρ meson

the σ matrices (from either the DA or the GPD) do not kill it anymore!

Is QCD factorisaton really justified?

- Recently, factorisation has been proved for the process $\pi^{\pm} N \to \gamma\gamma N'$ by Qiu, Yu [2205.07846].
- This was extended to a wide range of $2 \to 3$ exclusive processes by Qiu, Yu [2210.07995]

Is QCD factorisaton really justified?

- Recently, factorisation has been proved for the process $\pi^{\pm} N \to \gamma\gamma N'$ by Qiu, Yu [2205.07846].
- This was extended to a wide range of $2 \to 3$ exclusive processes by Qiu, Yu [2210.07995]
- The proof relies on having large p_T, rather than large invariant mass (e.g. photon-meson pair).

Is QCD factorisaton really justified?

- Recently, factorisation has been proved for the process $\pi^{\pm} N \to \gamma\gamma N'$ by Qiu, Yu [2205.07846].
- This was extended to a wide range of $2 \to 3$ exclusive processes by Qiu, Yu [2210.07995]
- The proof relies on having large p_T, rather than large invariant mass (e.g. photon-meson pair).
- In fact, NLO computation has been performed for $\gamma N \to \gamma\gamma N'$ by Grocholski, Pire, Sznajder, Szymanowski, Wagner [2110.00048].
- Also, NLO computation for $\gamma\gamma \to \pi^+\pi^-$ by crossing symmetry (but involves DAs only) by Duplancic, Nizic [hep-ph/0607069].

$$\gamma(q) + N(p_1) \to \gamma(k) + M(p_M, \varepsilon_M) + N'(p_2)$$

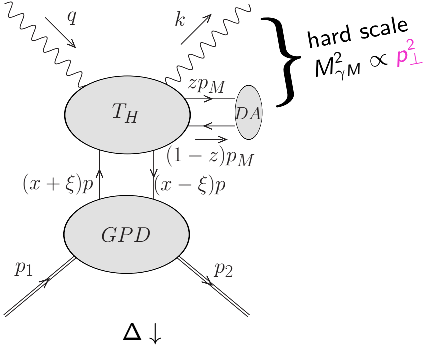

Useful Mandelstam variables:

$$t = (p_2 - p_1)^2$$

$$u' = (p_M - q)^2$$

$$t' = (k - q)^2$$

- Factorisation requires:
  $-u' > 1\ \mathrm{GeV}^2$, $-t' > 1\ \mathrm{GeV}^2$ and $(-t)_{\min} \leqslant -t \leqslant .5\ \mathrm{GeV}^2$

  $\implies$ sufficient to ensure large p_T.

Computation
Kinematics

$$\gamma(q) + N(p_1) \to \gamma(k) + M(p_M, \varepsilon_M) + N'(p_2)$$

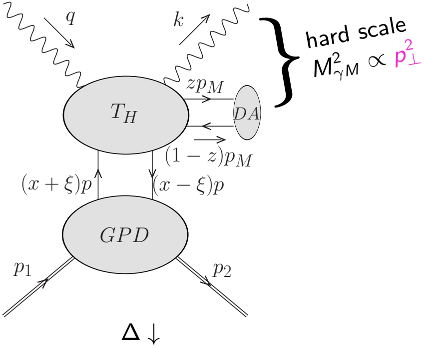

Useful Mandelstam variables:

$$t = (p_2 - p_1)^2$$

$$u' = (p_M - q)^2$$

$$t' = (k - q)^2$$

- Factorisation requires:
  $-u' > 1\ \mathrm{GeV}^2$, $-t' > 1\ \mathrm{GeV}^2$ and $(-t)_{\mathrm{min}} \leqslant -t \leqslant .5\ \mathrm{GeV}^2$
  $\Longrightarrow$ sufficient to ensure large p_T.
- Cross-section differential in $(-u')$ and $M^2_{\gamma M}$, and evaluated at $(-t) = (-t)_{\mathrm{min}}$.

$$\mathcal{A} = \int_{-1}^{1} dx \int_{0}^{1} dz \ T(x,\xi,z) \ H(x,\xi,t) \ \Phi_M(z)$$

$$\mathcal{A} = \int_{-1}^{1} dx \int_{0}^{1} dz \; T(x,\xi,z) \; H(x,\xi,t) \; \Phi_M(z)$$

- Differential cross section:

$$\left.\frac{d\sigma}{dt\, du'\, dM^2_{\gamma M}}\right|_{-t=(-t)_{min}} = \frac{|\overline{\mathcal{A}}|^2}{32 S^2_{\gamma N} M^2_{\gamma M} (2\pi)^3} \,.$$

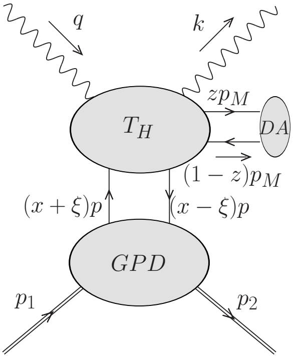

$$\mathcal{A} = \int_{-1}^{1} dx \int_{0}^{1} dz \; T(x,\xi,z) \; H(x,\xi,t) \; \Phi_M(z)$$

- Differential cross section:

$$\left.\frac{d\sigma}{dt\,du'\,dM^2_{\gamma M}}\right|_{-t=(-t)_{min}} = \frac{|\overline{\mathcal{A}}|^2}{32 S^2_{\gamma N} M^2_{\gamma M} (2\pi)^3} \,.$$

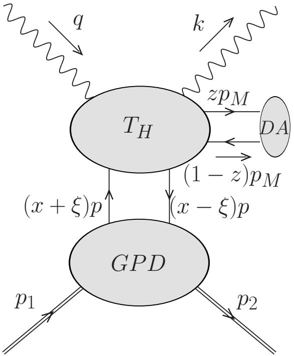

- Kinematic parameters: $S_{\gamma N}$, $M^2_{\gamma M}$, $-t$, $-u'$
- Useful dimensionless variables (hard part):

$$\alpha = \frac{-u'}{M^2_{\gamma M}} \,,$$

$$\xi = \frac{M^2_{\gamma M}}{2\,(S_{\gamma N} - m^2_N) - M^2_{\gamma M}} \,.$$

Quark GPDs are parametrised in terms of Double Distributions
[Radyushkin: hep-ph/9805342]

Quark GPDs are parametrised in terms of Double Distributions [Radyushkin: hep-ph/9805342]

For polarised PDFs (and hence transversity PDFs), two scenarios are proposed for the parameterization:

- "standard" scenario, with flavor-symmetric light sea quark and antiquark distributions.
- "valence" scenario with a completely flavor-asymmetric light sea quark densities.

Computation
DAs used

- We take the simplistic asymptotic form of the DAs

$$\phi_{\mathrm{as}}(z) = 6z(1-z)\,.$$

- We take the simplistic asymptotic form of the DAs

$$\phi_{\mathrm{as}}(z) = 6z(1-z)\,.$$

- We also investigate the effect of using a holographic DA:

$$\phi_{\mathrm{hol}}(z) = \frac{8}{\pi}\sqrt{z(1-z)}\,.$$

Suggested by

- AdS/QCD correspondence [Brodsky, de Teramond: hep-ph/0602252],
- dynamical chiral symmetry breaking on the light-front [Shi, Chen, Chang, Roberts, Schmidt, Zong: 1504.00689],
- recent lattice results. [Gao, Hanlon, Karthik, Mukherjee, Petreczky, Scior, Syritsyn, Zhao: 2206.04084]

Exclusive photoproduction of $\pi^0\gamma$

Gluonic GPD contributions

- Because of the quantum numbers of π^0 ($J^{PC} = 0^{-+}$), the exclusive photoproduction of $\pi^0\gamma$ is also sensitive to gluonic GPD contributions.

Exclusive photoproduction of $\pi^0\gamma$

Gluonic GPD contributions

- Because of the quantum numbers of π^0 ($J^{PC} = 0^{-+}$), the exclusive photoproduction of $\pi^0\gamma$ is also sensitive to gluonic GPD contributions.
- A total of 24 diagrams contribute in this case (compared to 20 diagrams from quark GPD contributions), with 6 groups of 4 related by symmetries ($x \to -x$ and $z \to 1 - z$ separately).

Exclusive photoproduction of $\pi^0\gamma$

Gluonic GPD contributions

- Because of the quantum numbers of π^0 ($J^{PC} = 0^{-+}$), the exclusive photoproduction of $\pi^0\gamma$ is also sensitive to gluonic GPD contributions.
- A total of 24 diagrams contribute in this case (compared to 20 diagrams from quark GPD contributions), with 6 groups of 4 related by symmetries ($x \to -x$ and $z \to 1 - z$ separately).
- Diagrams amount to connecting photons to the following two topologies.

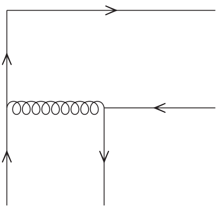

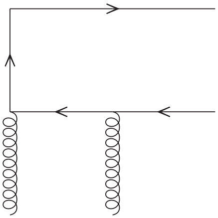

Exclusive photoproduction of $\pi^0\gamma$

Gluonic GPD contributions

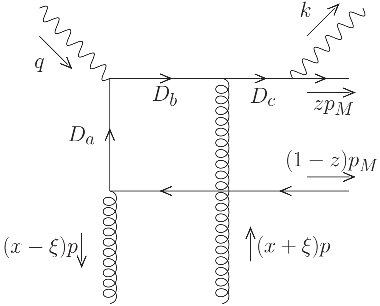

$$D_a = ((x-\xi)p + \bar{z}p_M)^2 + i\epsilon$$
$$= s\bar{\alpha}\bar{z}\left[\, x - \xi + i\epsilon \,\right] ,$$

$$D_b = (k + zp_M - (x+\xi)p)^2 + i\epsilon$$
$$= -s\left[z\left(x - \xi - i\epsilon \right) + \alpha\bar{z}\,(x + \xi - i\epsilon)\right] ,$$

$$D_c = (k + zp_M)^2 + i\epsilon$$
$$= 2s\xi z + i\epsilon$$

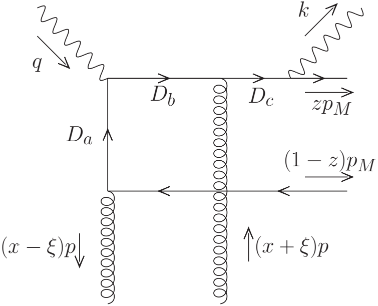

$$D_a = ((x-\xi)p + \bar{z}p_M)^2 + i\epsilon$$
$$= s\bar{\alpha}\bar{z}\left[x - \xi + i\epsilon\right] ,$$

$$D_b = (k + zp_M - (x+\xi)p)^2 + i\epsilon$$
$$= -s\left[z\left(x - \xi - i\epsilon\right) + \alpha\bar{z}\,(x + \xi - i\epsilon)\right] ,$$

$$D_c = (k + zp_M)^2 + i\epsilon$$
$$= 2s\xi z + i\epsilon$$

$\Longrightarrow$ *pinching of poles in the propagators in the limit of* $z \to 1$

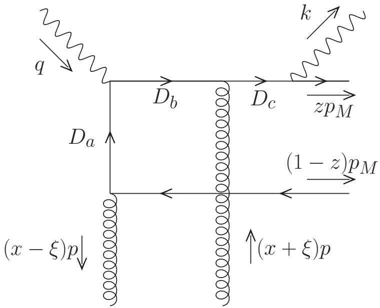

$$D_a = ((x-\xi)p + \bar{z}p_M)^2 + i\epsilon$$
$$= s\bar{\alpha}\bar{z}\left[x - \xi + i\epsilon\right] ,$$

$$D_b = (k + zp_M - (x+\xi)p)^2 + i\epsilon$$
$$= -s\left[z\left(x - \xi - i\epsilon\right) + \alpha\bar{z}\,(x + \xi - i\epsilon)\right] ,$$

$$D_c = (k + zp_M)^2 + i\epsilon$$
$$= 2s\xi z + i\epsilon$$

$\Longrightarrow$ *pinching of poles in the propagators in the limit of $z \to 1$*

Assuming an asymptotic form of the DA, they manifest themselves (*as a purely imaginary part*) in terms of

- $\int_0^1 \frac{dz}{z\bar{z}}$ contributions, when the x integration is performed first,
- $\int_1^1 dx \frac{\ln(x-\xi-i\epsilon)}{(x-\xi+i\epsilon)}$ contributions, when the z integration is performed first.

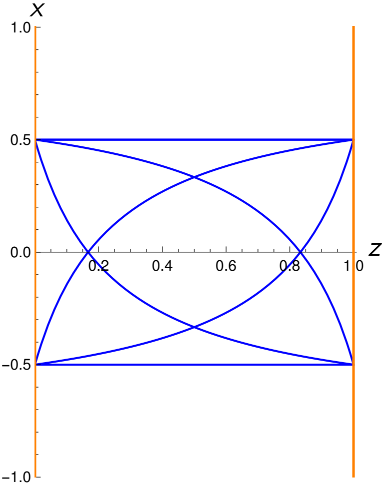

- Unfortunately, no cancellations between the 4 corners.

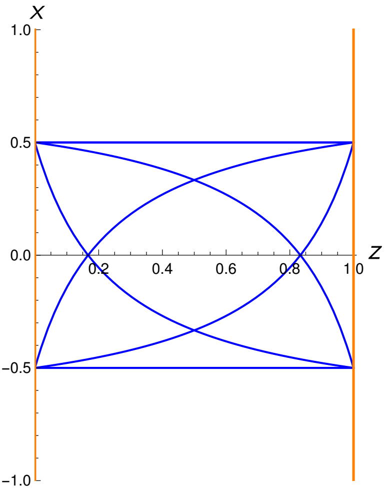

- Unfortunately, no cancellations between the 4 corners.
- Problem also shows up in $\pi^0 N \to \gamma\gamma N$.

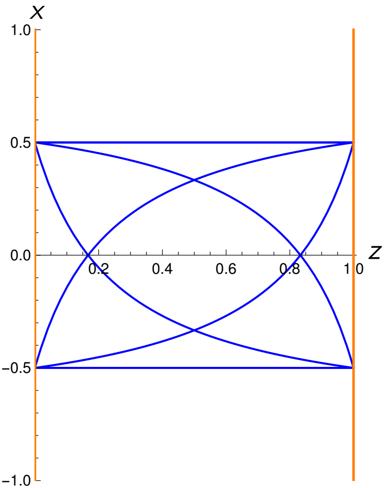

- Unfortunately, no cancellations between the 4 corners.
- Problem also shows up in $\pi^0 N \to \gamma\gamma N$.
- In $\gamma\gamma \to \pi^+\pi^-$, only ERBL region exists, no poles are crossed, and endpoint contributions are suppressed by DAs.

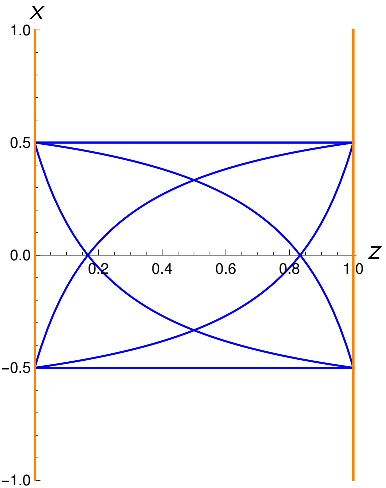

- Unfortunately, no cancellations between the 4 corners.
- Problem also shows up in $\pi^0 N \to \gamma\gamma N$.
- In $\gamma\gamma \to \pi^+\pi^-$, only ERBL region exists, no poles are crossed, and endpoint contributions are suppressed by DAs.
- As far as we know, this represents the first indication of violation of factorisation at leading order and twist-2.

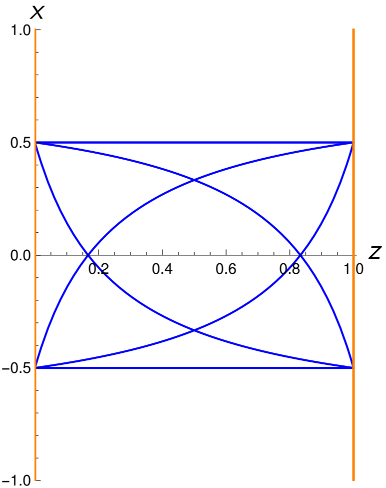

- Unfortunately, no cancellations between the 4 corners.
- Problem also shows up in $\pi^0 N \to \gamma\gamma N$.
- In $\gamma\gamma \to \pi^+\pi^-$, only ERBL region exists, no poles are crossed, and endpoint contributions are suppressed by DAs.
- As far as we know, this represents the first indication of violation of factorisation at leading order and twist-2.

- Problem happens only if both limits are taken, since singularity is a point in the integration region of momentum fractions.

[Details of phase space integration in backup]

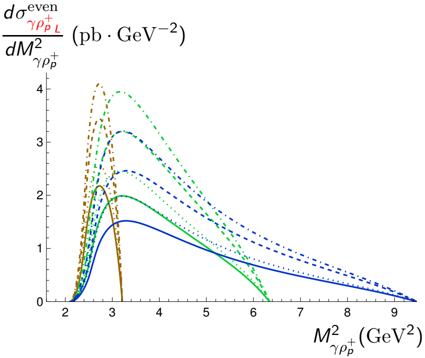

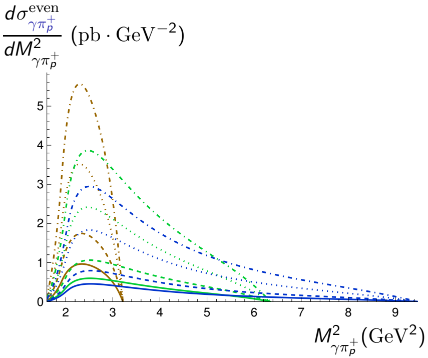

$S_{\gamma N} = 8,\ 14,\ 20\ \text{GeV}^2$

Dashed: Holographic DA   non-dashed: Asymptotical DA

Dotted: standard scenario   non-dotted: valence scenario

Results

Single differential cross-section: $\gamma\rho^+_{p\,L}$ vs $\gamma\pi^+_p$

[Details of phase space integration in backup]

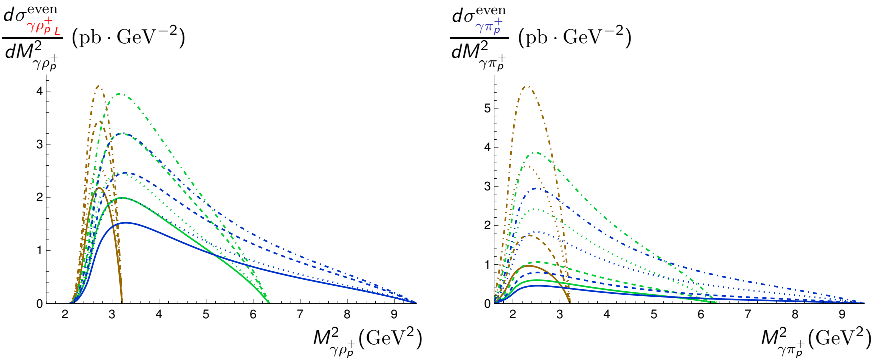

$$S_{\gamma N} = 8,\ 14,\ 20\ \text{GeV}^2$$

Dashed: Holographic DA non-dashed: Asymptotical DA

Dotted: standard scenario non-dotted: valence scenario

$\Longrightarrow$ Effect of GPD model more important on π^+_p than on ρ^+_p

Results

Single differential cross-section: $\gamma\rho^+_{p\,L}$ vs $\gamma\rho^+_{p\,T}$

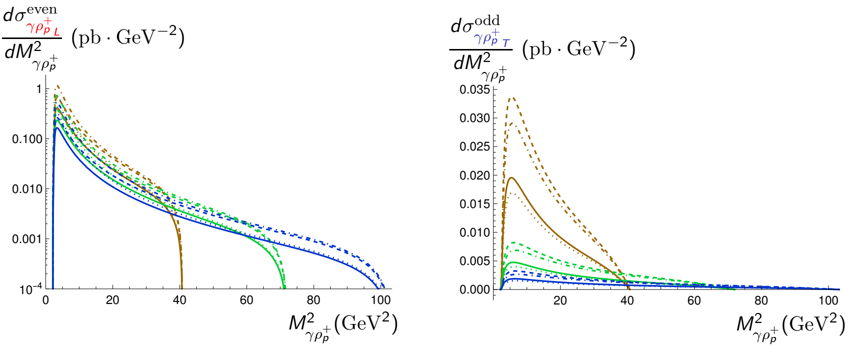

$S_{\gamma N} = 80, 140, 200$ GeV^2

Dashed: Holographic DA non-dashed: Asymptotical DA

Dotted: standard scenario non-dotted: valence scenario

Results

Single differential cross-section: $\gamma\rho^+_{p\,L}$ vs $\gamma\rho^+_{p\,T}$

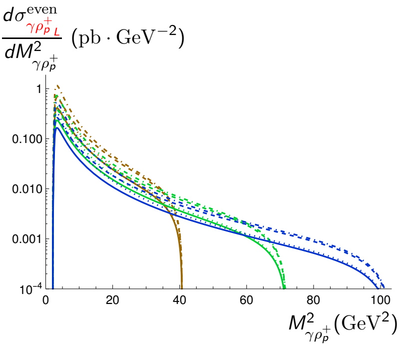

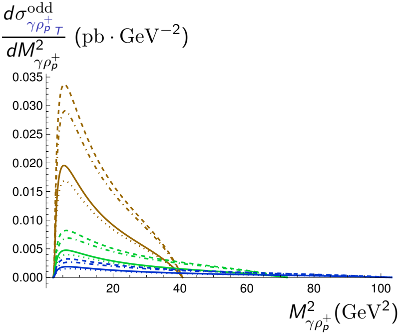

$S_{\gamma N} = 80, 140, 200$ GeV^2

Dashed: Holographic DA non-dashed: Asymptotical DA

Dotted: standard scenario non-dotted: valence scenario

CO cross-section is suppressed by a factor of ξ^2 ($\xi \approx \frac{M^2_{\gamma\rho}}{2S_{\gamma N}}$):
Measurable at small $S_{\gamma N}$, but drops rapidly with increasing $S_{\gamma N}$.

Results

Integrated cross-section: $\gamma\pi_p^+$ vs $\gamma\pi_n^-$

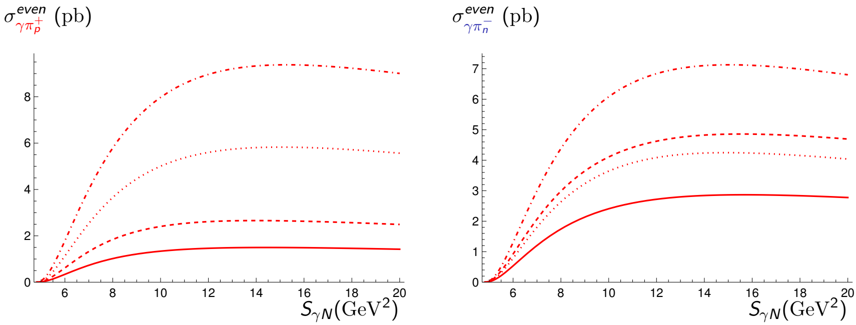

Dashed: Holographic DA   non-dashed: Asymptotical DA

Dotted: standard scenario   non-dotted: valence scenario

Integrated cross-section: $\gamma\pi_p^+$ vs $\gamma\pi_n^-$

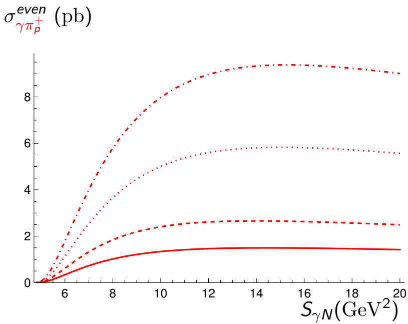

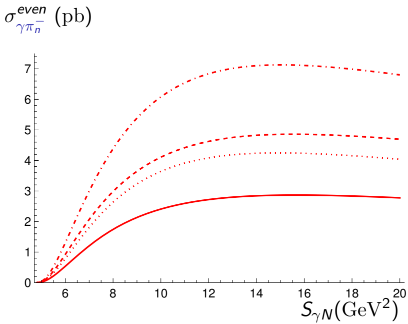

Dashed: Holographic DA non-dashed: Asymptotical DA

Dotted: standard scenario non-dotted: valence scenario

$\Longrightarrow$ Huge effect from GPD model in π_p^+ case.

Results

Integrated cross-section: $\gamma\rho^+_{P\,L}$ vs $\gamma\rho^+_{P\,T}$

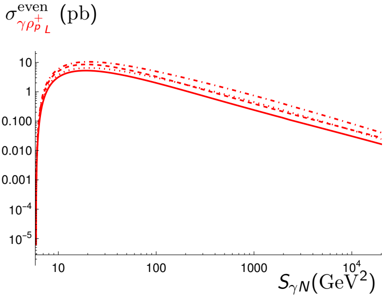

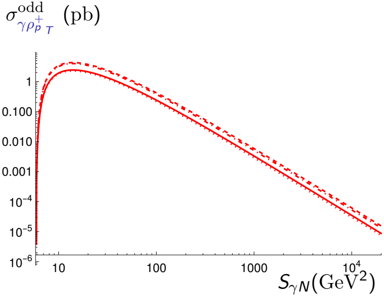

Dashed: Holographic DA non-dashed: Asymptotical DA

Dotted: standard scenario non-dotted: valence scenario

$\Longrightarrow$ ξ^2 suppression in the chiral-odd case causes the cross-section to drop rapidly with $S_{\gamma N}$.

We consider an unpolarised target, and determine polarisation asymmetries wrt the incoming photon.

We consider an unpolarised target, and determine polarisation asymmetries wrt the incoming photon.

- Circular polarisation asymmetry $= 0$.
- Linear polarisation asymmetry, LPA $= \frac{d\sigma_x - d\sigma_y}{d\sigma_x + d\sigma_y}$, where x is the direction defined by $p_\perp$ (direction of outgoing photon in the transverse plane).

We consider an unpolarised target, and determine polarisation asymmetries wrt the incoming photon.

- Circular polarisation asymmetry $= 0$.
- Linear polarisation asymmetry, LPA $= \frac{d\sigma_x - d\sigma_y}{d\sigma_x + d\sigma_y}$, where x is the direction defined by $p_\perp$ (direction of outgoing photon in the transverse plane).
- In fact,

$$\mathrm{LPA}_{\mathrm{Lab}} = \mathrm{LPA}\cos(2\theta) \ ,$$

where θ is the angle between the lab frame x-direction and $p_\perp$.

We consider an unpolarised target, and determine polarisation asymmetries wrt the incoming photon.

- Circular polarisation asymmetry $= 0$.
- Linear polarisation asymmetry, LPA $= \frac{d\sigma_x - d\sigma_y}{d\sigma_x + d\sigma_y}$, where x is the direction defined by $p_\perp$ (direction of outgoing photon in the transverse plane).
- In fact,

$$\mathrm{LPA}_{\mathrm{Lab}} = \mathrm{LPA}\cos(2\theta) \ ,$$

  where θ is the angle between the lab frame x-direction and $p_\perp$.
- Kleiss-Sterling spinor techniques used to obtain expressions.
- Both asymmetries zero in chiral-odd case!

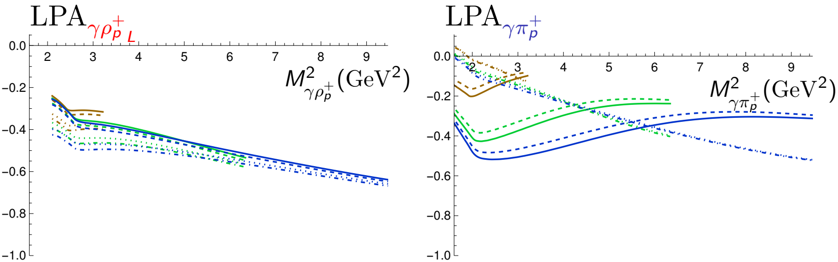

$S_{\gamma N} = 8,\ 14,\ 20\ \mathrm{GeV}^2$

Dashed: Holographic DA non-dashed: Asymptotical DA

Dotted: standard scenario non-dotted: valence scenario

LPA wrt incoming photon: Single-differential level: $\gamma\rho^+_{p\,L}$ vs $\gamma\pi^+_p$

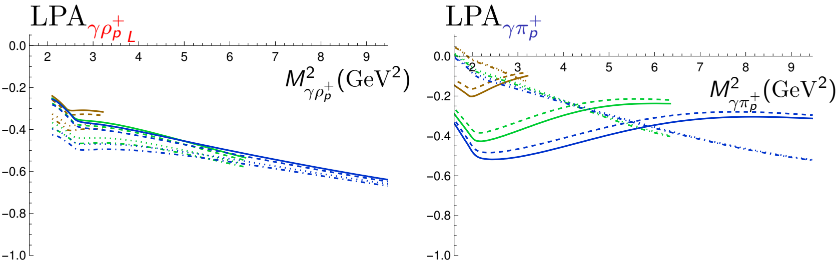

$$S_{\gamma N} = 8,\ 14,\ 20\ \mathrm{GeV}^2$$

Dashed: Holographic DA non-dashed: Asymptotical DA

Dotted: standard scenario non-dotted: valence scenario

$\Longrightarrow$ GPD model changes the behaviour of the LPA completely in the π^+_p case!

Good statistics: For example, at JLab Hall B:

- untagged incoming $\gamma \Rightarrow$ Weizsäcker-Williams distribution

Good statistics: For example, at JLab Hall B:

- untagged incoming $\gamma \Rightarrow$ Weizsäcker-Williams distribution
- with an expected luminosity of $\mathcal{L} = 100\ \mathrm{nb}^{-1} s^{-1}$, for 100 days of run:
  - ρ_L^0 (on p) : $\approx 2.4 \times 10^5$
  - ρ_T^0 (on p) : $\approx 4.2 \times 10^4$ (Chiral-odd)
  - ρ_L^+ : $\approx 1.4 \times 10^5$
  - ρ_T^+ : $\approx 6.7 \times 10^4$ (Chiral-odd)
  - π^+ : $\approx 1.8 \times 10^5$

Good statistics: For example, at JLab Hall B:

- untagged incoming $\gamma \Rightarrow$ Weizsäcker-Williams distribution
- with an expected luminosity of $\mathcal{L} = 100\ \mathrm{nb}^{-1} s^{-1}$, for 100 days of run:
  - ρ_L^0 (on p) : $\approx 2.4 \times 10^5$
  - ρ_T^0 (on p) : $\approx 4.2 \times 10^4$ (Chiral-odd)
  - ρ_L^+ : $\approx 1.4 \times 10^5$
  - ρ_T^+ : $\approx 6.7 \times 10^4$ (Chiral-odd)
  - π^+ : $\approx 1.8 \times 10^5$
- No problem in detecting outgoing photon at JLab [backup].

At COMPASS:

- Taking a luminosity of $\mathcal{L} = 0.1\ \mathrm{nb}^{-1} s^{-1}$, and 300 days of run,
  - ρ_L^0 (on p) : $\approx 1.2 \times 10^3$
  - ρ_T^0 (on p) : $\approx 1.5 \times 10^2$ (Chiral-odd)
  - ρ_L^+ : $\approx 7.4 \times 10^2$
  - ρ_T^+ : $\approx 2.6 \times 10^2$ (Chiral-odd)
  - π^+ : $\approx 7.4 \times 10^2$

At COMPASS:

- Taking a luminosity of $\mathcal{L} = 0.1\ \mathrm{nb}^{-1} s^{-1}$, and 300 days of run,
  - ρ_L^0 (on p) : $\approx 1.2 \times 10^3$
  - ρ_T^0 (on p) : $\approx 1.5 \times 10^2$ (Chiral-odd)
  - ρ_L^+ : $\approx 7.4 \times 10^2$
  - ρ_T^+ : $\approx 2.6 \times 10^2$ (Chiral-odd)
  - π^+ : $\approx 7.4 \times 10^2$
- Lower numbers due to low luminosity (factor of 10^3 less than JLab!)

Prospects at experiments

Counting rates: EIC

- At the future EIC, with an expected integrated luminosity of $10\,\mathrm{fb}^{-1}$ (about 100 times smaller than JLab):
  - ρ_L^0 (on p) : $\approx 2.4 \times 10^4$
  - ρ_T^0 (on p) : $\approx 2.4 \times 10^3$ (Chiral-odd)
  - ρ_L^+ : $\approx 1.5 \times 10^4$
  - ρ_T^+ : $\approx 4.2 \times 10^3$ (Chiral-odd)
  - π^+ : $\approx 1.3 \times 10^4$

- At the future EIC, with an expected integrated luminosity of $10\,\mathrm{fb}^{-1}$ (about 100 times smaller than JLab):
  - ρ_L^0 (on p) : $\approx 2.4 \times 10^4$
  - ρ_T^0 (on p) : $\approx 2.4 \times 10^3$ (Chiral-odd)
  - ρ_L^+ : $\approx 1.5 \times 10^4$
  - ρ_T^+ : $\approx 4.2 \times 10^3$ (Chiral-odd)
  - π^+ : $\approx 1.3 \times 10^4$
- Small ξ study:
  $300 < S_{\gamma N}/\,\mathrm{GeV}^2 < 20000$ ($5 \cdot 10^{-5} < \xi < 5 \cdot 10^{-3}$):
  - ρ_L^0 (on p) : $\approx 1.2 \times 10^3$
  - ρ_T^0 (on p) : ≈ 6.5 (Chiral-odd) (tiny)
  - ρ_L^+ : $\approx 9.3 \times 10^2$
  - π^+ : $\approx 5.0 \times 10^2$

For p-Pb UPCs at LHC (integrated luminosity of 1200 nb^{-1}):

- With future data from runs 3 and 4,
  - $\rho_L^0 : \approx 1.6 \times 10^4$
  - $\rho_T^0 : \approx 1.7 \times 10^3$ (Chiral-odd)
  - $\rho_L^+ : \approx 1.1 \times 10^4$
  - $\rho_T^+ : \approx 2.9 \times 10^3$ (Chiral-odd)
  - $\pi^+ : \approx 9.3 \times 10^3$

For p-Pb UPCs at LHC (integrated luminosity of 1200 nb^{-1}):

- With future data from runs 3 and 4,
  - $\rho_L^0 : \approx 1.6 \times 10^4$
  - $\rho_T^0 : \approx 1.7 \times 10^3$ (Chiral-odd)
  - $\rho_L^+ : \approx 1.1 \times 10^4$
  - $\rho_T^+ : \approx 2.9 \times 10^3$ (Chiral-odd)
  - $\pi^+ : \approx 9.3 \times 10^3$
- $300 < S_{\gamma N}/\,\text{GeV}^2 < 20000$ ($5 \cdot 10^{-5} < \xi < 5 \cdot 10^{-3}$):
  - $\rho_L^0 : \approx 8.1 \times 10^2$
  - $\rho_L^+ : \approx 6.4 \times 10^2$
  - $\pi^+ : \approx 3.4 \times 10^2$

Conclusion

- Exclusive photoproduction of photon-meson pair provides additional channel for extracting GPDs, which are essential for nucleon tomography.

Conclusion

- Exclusive photoproduction of photon-meson pair provides additional channel for extracting GPDs, which are essential for nucleon tomography.
- Especially interesting since it can probe chiral-odd GPDs at the leading twist, and provides better sensitivity to x-dependence of GPDs.

Conclusion

- Exclusive photoproduction of photon-meson pair provides additional channel for extracting GPDs, which are essential for nucleon tomography.
- Especially interesting since it can probe chiral-odd GPDs at the leading twist, and provides better sensitivity to x-dependence of GPDs.
- Proof of factorisation for this family of processes now available, but intriguing indication of violation of collinear factorisation at twist-2 with gluonic contributions to $\pi^0\gamma$ photoproduction.

Conclusion

- Exclusive photoproduction of photon-meson pair provides additional channel for extracting GPDs, which are essential for nucleon tomography.
- Especially interesting since it can probe chiral-odd GPDs at the leading twist, and provides better sensitivity to x-dependence of GPDs.
- Proof of factorisation for this family of processes now available, but intriguing indication of violation of collinear factorisation at twist-2 with gluonic contributions to $\pi^0\gamma$ photoproduction.
- Good statistics in various experiments, particularly at JLab.

Conclusion

- Exclusive photoproduction of photon-meson pair provides additional channel for extracting GPDs, which are essential for nucleon tomography.
- Especially interesting since it can probe chiral-odd GPDs at the leading twist, and provides better sensitivity to x-dependence of GPDs.
- Proof of factorisation for this family of processes now available, but intriguing indication of violation of collinear factorisation at twist-2 with gluonic contributions to $\pi^0\gamma$ photoproduction.
- Good statistics in various experiments, particularly at JLab.
- Small ξ limit of GPDs can be investigated by exploiting high energies available in collider mode such as EIC and UPCs at LHC.

Outlook

- $\gamma N \to \gamma \pi^0 N$ is of particular interest, since they give access to gluonic GPDs at LO [ongoing]:
  - Issue with endpoint singularities

Outlook

- $\gamma N \to \gamma\pi^0 N$ is of particular interest, since they give access to gluonic GPDs at LO [ongoing]:
  - Issue with endpoint singularities
- Compute NLO corrections: [ongoing]
  - Quark GPD contribution only involves 422 diagrams!
  - Also, double integration over momentum fractions: Very hard!

Outlook

- $\gamma N \to \gamma \pi^0 N$ is of particular interest, since they give access to gluonic GPDs at LO [ongoing]:
  - Issue with endpoint singularities
- Compute NLO corrections: [ongoing]
  - Quark GPD contribution only involves 422 diagrams!
  - Also, double integration over momentum fractions: Very hard!
- Generalise to electroproduction ($Q^2 \neq 0$).
- Add Bethe-Heitler component (photon emitted from incoming lepton)
  - zero in chiral-odd case.
  - suppressed in chiral-even case.

BACKUP SLIDES

A total of 20 diagrams to compute

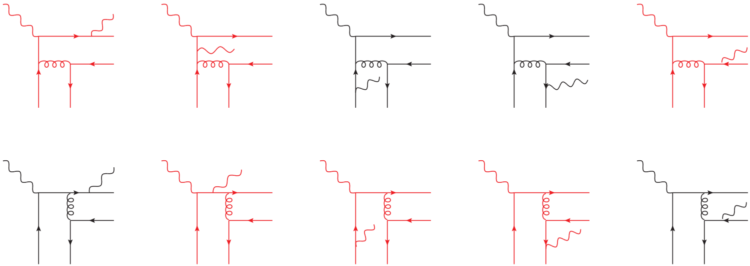

- Need to compute 10 diagrams: Other half related by $q \leftrightarrow \bar{q}$ (anti)symmetry.
- In fact, by choosing the right gauge, only 4 diagrams can be used to generate all the others by various symmetries (eg. photon exchange).
- Red diagrams cancel in the chiral-odd case

$$\int \frac{dz^-}{4\pi} e^{ixP^+z^-} \langle p_2, \lambda_2 | \bar{\psi}_q \left(-\frac{1}{2}z^-\right) \gamma^+ \psi \left(\frac{1}{2}z^-\right) | p_1, \lambda_1 \rangle$$

$$= \frac{1}{2P^+} \bar{u}(p_2, \lambda_2) \left[H^q(x, \xi, t) \gamma^+ + E^q(x, \xi, t) \frac{i\sigma^{\alpha+}\Delta_\alpha}{2m} \right] u(p_1, \lambda_1)$$

$$\int \frac{dz^-}{4\pi} e^{ixP^+z^-} \langle p_2, \lambda_2 | \bar{\psi}_q \left(-\frac{1}{2}z^-\right) \gamma^+ \gamma^5 \psi \left(\frac{1}{2}z^-\right) | p_1, \lambda_1 \rangle$$

$$= \frac{1}{2P^+} \bar{u}(p_2, \lambda_2) \left[\tilde{H}^q(x, \xi, t) \gamma^+ \gamma^5 + \tilde{E}^q(x, \xi, t) \frac{\gamma^5 \Delta^+}{2m} \right] u(p_1, \lambda_1)$$

- Take the limit $\Delta_\perp = 0$.
- In that case and for small ξ, the dominant contributions come from H^q and $\tilde{H}^q$.

$$
\begin{aligned}
&\int \frac{dz^-}{4\pi} e^{ixP^+z^-} \langle p_2, \lambda_2 | \bar{\psi}_q \left(-\frac{1}{2}z^-\right) i\sigma^{+i} \psi \left(\frac{1}{2}z^-\right) | p_1, \lambda_1 \rangle \\
= \;& \frac{1}{2P^+} \bar{u}(p_2, \lambda_2) \Bigg[H_T^q(x,\xi,t) i\sigma^{+i} + \tilde{H}_T^q(x,\xi,t) \frac{P^+\Delta^i - \Delta^+ P^i}{m_N^2} \\
+ \;& E_T^q(x,\xi,t) \frac{\gamma^+\Delta^i - \Delta^+\gamma^i}{2m_N} + \tilde{E}_T^q(x,\xi,t) \frac{\gamma^+ P^i - P^+\gamma^i}{m_N} \Bigg] u(p_1, \lambda_1)
\end{aligned}
$$

- Take the limit $\Delta_\perp = 0$.
- In that case and for small ξ, the dominant contributions come from H_T^q.

- GPDs can be represented in terms of Double Distributions
  [Radyushkin: hep-ph/9805342]

$$H^q(x,\xi,t=0) = \int_{-1}^{1} d\beta \int_{-1+|\beta|}^{1-|\beta|} d\alpha\ \delta(\beta+\xi\alpha-x)\, f^q(\beta,\alpha)$$

- ansatz for these Double Distributions:
  - chiral-even sector:

$$f^q(\beta,\alpha,t=0) = \Pi(\beta,\alpha)\, q(\beta)\Theta(\beta) - \Pi(-\beta,\alpha)\, \bar{q}(-\beta)\, \Theta(-\beta)\,,$$
$$\tilde{f}^q(\beta,\alpha,t=0) = \Pi(\beta,\alpha)\, \Delta q(\beta)\Theta(\beta) + \Pi(-\beta,\alpha)\, \Delta\bar{q}(-\beta)\, \Theta(-\beta)\,.$$

  - chiral-odd sector:

$$f^q_T(\beta,\alpha,t=0) = \Pi(\beta,\alpha)\, \delta q(\beta)\Theta(\beta) - \Pi(-\beta,\alpha)\, \delta\bar{q}(-\beta)\, \Theta(-\beta)\,.$$

  - $\Pi(\beta,\alpha) = \frac{3}{4}\frac{(1-\beta)^2-\alpha^2}{(1-\beta)^3}$: profile function

- simplistic factorised ansatz for the t-dependence:

$$H^q(x,\xi,t) = H^q(x,\xi,t=t_{\rm min}) \times F_H(t)$$

with $F_H(t) = \frac{(t_{\rm min}-C)^2}{(t-C)^2}$ a standard dipole form factor ($C = 0.71 \mathrm{GeV}^2$)

Sets of PDFs used to model GPDs

- $q(x)$: unpolarised PDF:
  - GRV-98 [Glück, Reya, Vogt: hep-ph/9806404]
  - MSTW2008lo [Martin, Stirling, Thorne, Watt: 0901.0002]
  - MSTW2008nnlo [Martin, Stirling, Thorne, Watt: 0901.0002]
  - ABM11nnlo [Alekhin, Blumlein, Moch: 1202.2281]
  - CT10nnlo [Gao, Guzzi, Huston, Lai, Li, Nadolsky, Pumplin, Stump, Yuan: 1302.6246]
- $\Delta q(x)$ polarised PDF
  - GRSV-2000 [Glück, Reya, Stratmann, Vogelsang: hep-ph/0011215]
- $\delta q(x)$: transversity PDF:
  - Based on parameterisation for TMDs from which transversity PDFs obtained as limiting case [Anselmino, Boglione, D'Alesio, Melis, Murgia, Prokudin: 1303.3822]

Effects are not significant! But relevant for NLO corrections!

- Helicity conserving (vector) DA at twist 2: ρ_L

$$\langle 0|\bar{u}(0)\gamma^\mu u(x)|\rho_L^0(p)\rangle = \frac{p^\mu}{\sqrt{2}} f_\rho \int_0^1 du\ e^{-iup\cdot x}\phi_\rho(u)$$

- Helicity flip (tensor) DA at twist 2: ρ_T

$$\langle 0|\bar{u}(0)\sigma^{\mu\nu} u(x)|\rho_T^0(p,s)\rangle = \frac{i}{\sqrt{2}}(\epsilon_\rho^\mu p^\nu - \epsilon_\rho^\nu p^\mu) f_\rho^\perp \int_0^1 du\ e^{-iup\cdot x}\ \phi_\rho(u)$$

- Helicity conserving (axial) DA at twist 2: $\pi^\pm$

$$\langle 0|\bar{u}(0)\gamma^\mu\gamma^5 d(x)|\pi(p)\rangle = ip^\mu f_\pi \int_0^1 du\ e^{-iup\cdot x}\phi_\pi(u)$$

Valence vs Standard scenarios in $\tilde{H}$ (Chiral-even, Axial)

Typical kinematic point (for JLab kinematics):
$\xi = .1 \ \leftrightarrow \ S_{\gamma N} = 20 \ \mathrm{GeV}^2$ and $M^2_{\gamma\rho} = 3.5 \ \mathrm{GeV}^2$

$$\tilde{H}^{q(-)}(x,\xi,t) = \tilde{H}^q(x,\xi,t) - \tilde{H}^q(-x,\xi,t) \quad [C = -1]$$

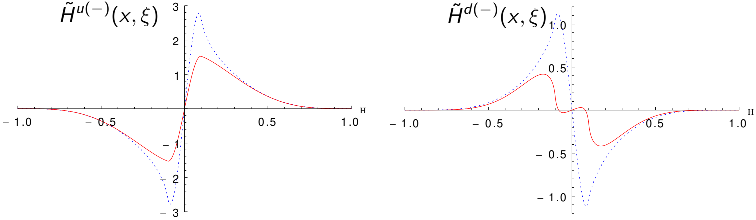

"valence" and "standard": two GRSV Ansätze for $\Delta q(x)$

Typical kinematic point (for JLab kinematics):
$\xi = .1 \;\leftrightarrow\; S_{\gamma N} = 20\ \mathrm{GeV}^2$ and $M^2_{\gamma\rho} = 3.5\ \mathrm{GeV}^2$

$$H_T^{q(-)}(x,\xi,t) = H_T^q(x,\xi,t) + H_T^q(-x,\xi,t) \quad [C=-1]$$

$H_T^{u(-)}(x,\xi)$

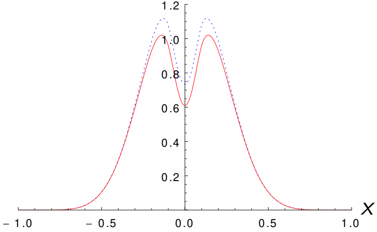

$H_T^{d(-)}(x,\xi)$

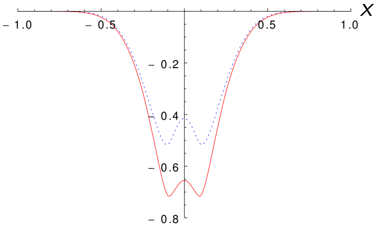

"valence" and "standard": two GRSV Ansätze for $\Delta q(x)$

$\Rightarrow$ two Ansätze for $\delta q(x)$

- Work in the limit of:
  - $\Delta_\perp \ll p_\perp$
  - $m_N^2,\ m_M^2 \ll M_{\gamma M}^2$
- initial state particle momenta:

$$q^\mu = n^\mu,$$
$$p_1^\mu = (1+\xi)\,p^\mu + \frac{m_N^2}{s(1+\xi)}n^\mu$$

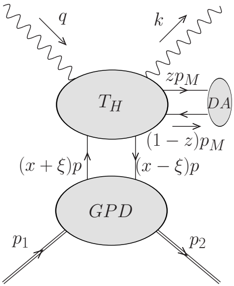

hard scale $M_{\gamma M}^2 \propto p_\perp^2$

- final state particle momenta:

$$p_2^\mu = (1-\xi)\,p^\mu + \frac{m_N^2+\vec{p}_t^{\,2}}{s(1-\xi)}n^\mu + \Delta_\perp^\mu$$

$$k^\mu = \alpha\, n^\mu + \frac{(\vec{p}_t - \vec{\Delta}_t/2)^2}{\alpha s}\,p^\mu + p_\perp^\mu - \frac{\Delta_\perp^\mu}{2}\,,$$

$\Delta \downarrow$

$$p_M^\mu = \alpha_M\, n^\mu + \frac{(\vec{p}_t + \vec{\Delta}_t/2)^2 + m_M^2}{\alpha_M s}\,p^\mu - p_\perp^\mu - \frac{\Delta_\perp^\mu}{2}\,,$$

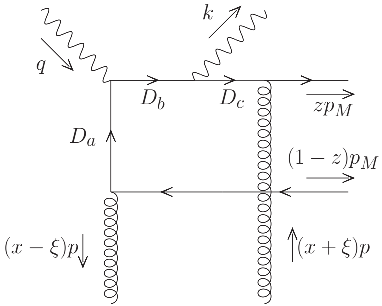

$$D_a = ((x-\xi)p + \bar{z}p_M)^2 + i\epsilon$$
$$= s\bar{\alpha}\bar{z}\left[x-\xi+i\epsilon\right] ,$$

$$D_b = (k + zp_M - (x+\xi)p)^2 + i\epsilon$$
$$= -s\left[z\left(x-\xi-i\epsilon\right) + \alpha\bar{z}\left(x+\xi-i\epsilon\right)\right] ,$$

$$D_c = (zp_M - (x+\xi)p)^2 + i\epsilon$$
$$= -s\bar{\alpha}z\left[x+\xi-i\epsilon\right]$$

$\Longrightarrow$ *pinching of poles in the propagators (D_a and D_b) in the limit of $z \to 1$*

Results

Fully-differential cross-sections: $\gamma\rho^+_{p\,L}$ vs $\gamma\rho^-_{n\,L}$

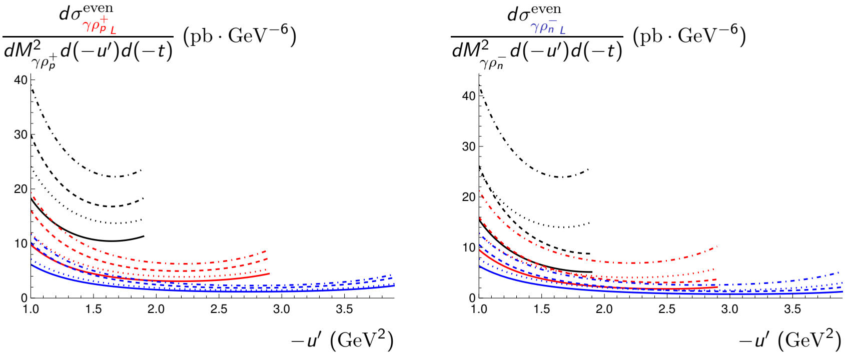

$$S_{\gamma N} = 20\ \text{GeV}^2,\ -t = (-t)_{\text{min}},\ M^2_{\gamma\rho} = 3, 4, 5\ \text{GeV}^2$$

Dashed: Holographic DA   non-dashed: Asymptotical DA

Dotted: standard scenario   non-dotted: valence scenario

large angle scattering: $M^2_{\gamma\rho} \sim -u' \sim -t' \quad (S_{\gamma N} = 20 \text{ GeV}^2)$

$\Longrightarrow -u' > 1 \text{ GeV}^2$ and $-t' > 1 \text{ GeV}^2$ and $(-t)_{\min} \leqslant -t \leqslant .5 \text{ GeV}^2$

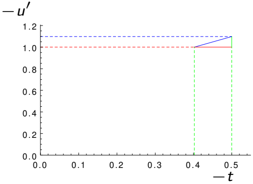

$M_{\gamma\rho} = 2.2 \text{ GeV}^2$

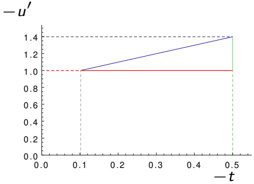

$M^2_{\gamma\rho} = 2.5 \text{ GeV}^2$

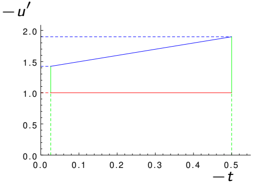

$M_{\gamma\rho} = 3 \text{ GeV}^2$

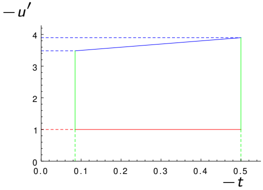

$M_{\gamma\rho} = 5 \text{ GeV}^2$

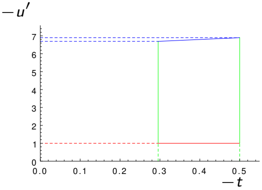

$M_{\gamma\rho} = 8 \text{ GeV}^2$

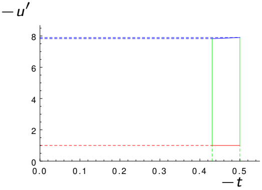

$M_{\gamma\rho} = 9 \text{ GeV}^2$

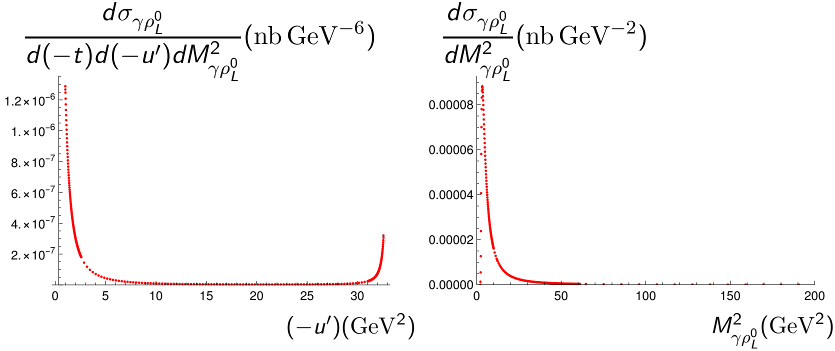

- Need enough points at boundaries for distribution in $(-u')$
- Need enough points to resolve peak (at low $M^2_{\gamma\rho_L^0}$) for distribution in $M^2_{\gamma\rho_L^0}$

Results

Explaining the difference between chiral-even and chiral-odd plots

- $\xi = \frac{M^2_{\gamma M}}{2S_{\gamma N} - M_N^2} \approx \frac{M^2_{\gamma M}}{2S_{\gamma N}}$ for $M^2_{\gamma M} \ll S_{\gamma N}$
- Chiral-even (unpolarised) cross-section:

$$|\overline{\mathcal{M}}_{\mathrm{CE}}|^2 = \frac{2}{s^2}(1-\xi^2)C_{\mathrm{CE}}^2 \left\{ 2\,|N_A|^2 + \frac{p_\perp^4}{s^2}\,|N_B|^2 + \frac{p_\perp^2}{s}\,(N_A N_B^* + c.c.) + \frac{p_\perp^4}{4s^2}\,|N_{A_5}|^2 + \frac{p_\perp^4}{4s^2}\,|N_{B_5}|^2 \right\}.$$

- Chiral-odd (unpolarised) cross-section:

$$|\overline{\mathcal{M}}_{CO}|^2 = \frac{2048}{s^2}\xi^2(1-\xi^2)C_{\mathrm{CO}}^2 \left\{ \alpha^4\,|N_{T\,A}|^2 + |N_{T\,B}|^2 \right\}.$$

- Note: $\alpha = \frac{-u'}{M^2_{\gamma M}}$.

To obtain distribution in $S_{\gamma N}$, we exploit non-trivial mapping between 1 set of data at a fixed $S_{\gamma N}$ to other values $\tilde{S}_{\gamma N}$ *lower* than it.

$$\tilde{M}^2_{\gamma M} = M^2_{\gamma M} \frac{\tilde{S}_{\gamma N} - m_N^2}{S_{\gamma N} - m_N^2},$$

$$-\tilde{u}' = \frac{\tilde{M}^2_{\gamma M}}{M^2_{\gamma M}}(-u').$$

Implementing importance sampling $\implies$ careful consideration of the various limits involved are needed.

Mapping possible since different sets of $(S_{\gamma N}, M^2_{\gamma M}, -u')$ correspond to the same (α, ξ).

$$\alpha = \frac{-u'}{M^2_{\gamma M}}, \qquad \xi = \frac{M^2_{\gamma M}}{2(S_{\gamma N} - m_N^2) - M^2_{\gamma M}}.$$

Consider

$$\gamma(q,\lambda_q) + N(p_1,\lambda_1) \to \gamma(k,\lambda_k) + \pi^{\pm}(p_\pi) + N'(p_2,\lambda_2)\ ,$$

where λ_i represent the helicities of the particles.

QED/QCD invariance under parity implies that [Bourrely, Soffer, Leader: Phys.Rept. 59 (1980) 95-297]

$$\mathcal{A}_{\lambda_2\lambda_k\,;\,\lambda_1\lambda_q} = \eta\,(-1)^{\lambda_1-\lambda_q-(\lambda_2-\lambda_k)}\mathcal{A}_{-\lambda_2-\lambda_k\,;\,-\lambda_1-\lambda_q}\ ,$$

where η represents phase factors related to intrinsic spin.

Thus, at the cross-section level, it is clear that circular asymmetry will vanish, since

$$\sum_{\lambda_i,\,i\neq q}\left|\mathcal{A}_{\lambda_2\lambda_k\,;\,\lambda_1+}\right|^2 = \sum_{\lambda_i,\,i\neq q}\left|\mathcal{A}_{\lambda_2\lambda_k\,;\,\lambda_1-}\right|^2$$

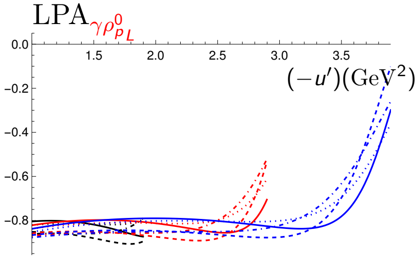

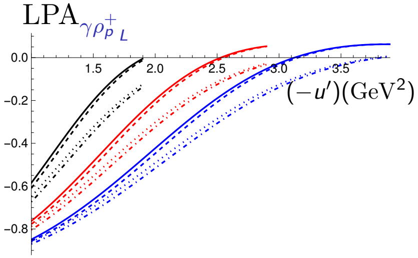

$$S_{\gamma N} = 20\ \mathrm{GeV}^2,\ -t = (-t)_{\mathrm{min}},\ M^2_{\gamma\rho} = 3, 4, 5\ \mathrm{GeV}^2$$

Dashed: Holographic DA non-dashed: Asymptotical DA

Dotted: standard scenario non-dotted: valence scenario

Results

LPA wrt incoming photon: Integrated level: $\gamma\rho^-_{n\ L}$ vs $\gamma\pi^-_n$

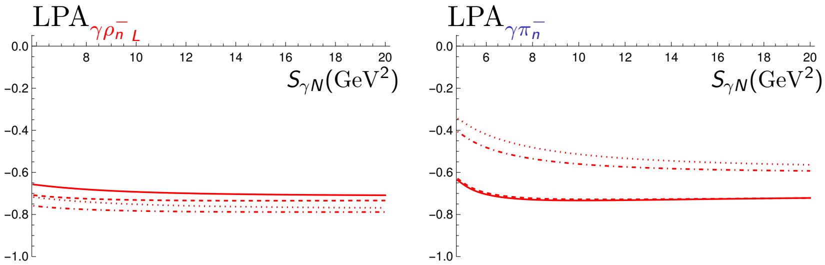

Dashed: Holographic DA non-dashed: Asymptotical DA

Dotted: standard scenario non-dotted: valence scenario

Why counting rates lower UPCs at LHC?

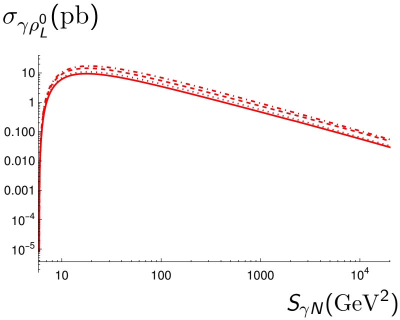

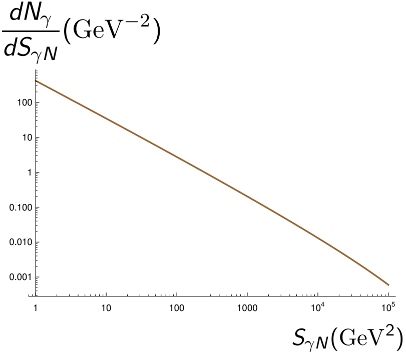

- Photon flux enhanced by a factor of Z^2, but drops rapidly with $S_{\gamma N} \Longrightarrow$ *Low luminosity not compensated by larger photon flux.*
- LHC great for high energy, but JLab better in terms of luminosity.
- Still, LHC gives us access to the small ξ region of GPDs!

Angular distribution: $\rho_p^0\gamma$ photoproduction at $S_{\gamma N} = 20\,\mathrm{GeV}^2$

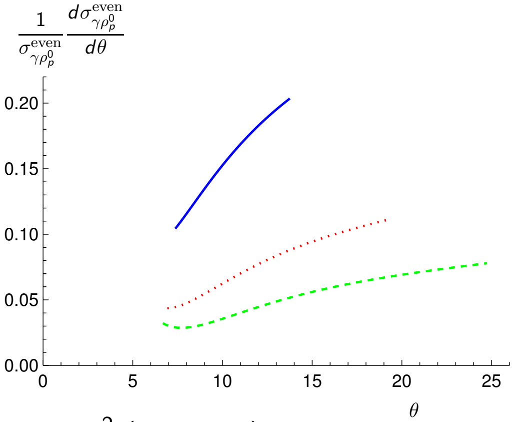

- $M^2_{\gamma\rho^0_p} = 4\ \mathrm{GeV}^2$ (solid blue)
- $M^2_{\gamma\rho^0_p} = 6\ \mathrm{GeV}^2$ (dotted red)
- $M^2_{\gamma\rho^0_p} = 8\ \mathrm{GeV}^2$ (dashed green)

Angular cuts on outgoing photon at JLab

Single differential cross-section: $\rho_p^0\gamma$ photoproduction at $S_{\gamma N} = 20\,\text{GeV}^2$

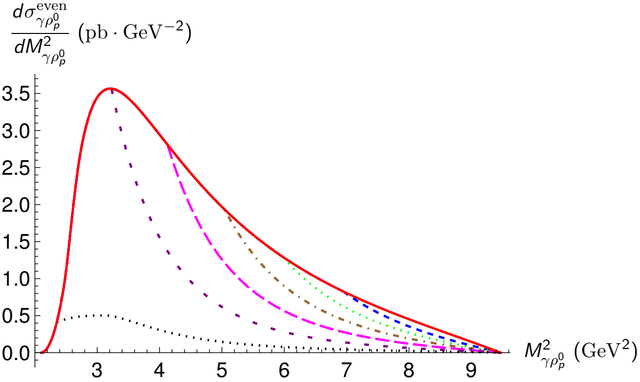

- no angular cut (solid red)
- $\theta \leq 35^\circ$ (dashed blue)
- $\theta \leq 30^\circ$ (dotted green)
- $\theta \leq 25^\circ$ (dashed-dotted brown)
- $\theta \leq 20^\circ$ (long-dashed magenta)
- $\theta \leq 15^\circ$ (short-dashed purple)
- $\theta \leq 10^\circ$ (dotted black)